

Graded potential wells with quasi-uniform charge distribution

Achim Wixforth, M. Sundaram, D. Donnelly, J.H. English, A.C. Gossard

Angaben zur Veröffentlichung / Publication details:

Wixforth, Achim, M. Sundaram, D. Donnelly, J.H. English, and A.C. Gossard. 1990. "Graded potential wells with quasi-uniform charge distribution." *Surface Science* 228 (1-3): 489–92.
[https://doi.org/10.1016/0039-6028\(90\)90360-k](https://doi.org/10.1016/0039-6028(90)90360-k).

GRADED POTENTIAL WELLS WITH QUASI-UNIFORM CHARGE DISTRIBUTION

A. WIXFORTH, M. SUNDARAM, D. DONNELLY, J.H. ENGLISH and A.C. GOSSARD

University of California, Santa Barbara, CA 93106, USA

We report on the growth and the characterization of several quasi-three-dimensional electron systems as realized in modulation-doped graded potential wells. We study the charge distribution, the subband structure, and the electronic properties of the samples by means of capacitance-voltage techniques as well as by the investigation of the cyclotron resonance at low temperatures. The results of our investigations are fed back into the growth conditions, which leads to the production of symmetrical, quasi-uniform charge distributions with three-dimensional properties.

There has been enormous progress in the production and the investigation of two-, one-, and even zero-dimensional electron systems in the last decade, but with the exception of superconductors, no comparable progress has been made in the three-dimensional case. A new growth technique [1,2], referred to in the following as the concept of quasi-doping, now has made it possible to artificially realize high quality quasi-three-dimensional electron systems (Q3DES) with electron mobilities in excess of $200\,000\text{ cm}^2\text{ V}^{-1}\text{ s}^{-1}$. Such structures reveal an approach to the hypothetical construct of jellium, a neutral medium consisting of an electron gas moving in the potential of a uniform positively charged background. Theoretical investigations of this construct predict a lot of interesting many-body effects [3], many of which have not yet been observed experimentally.

The concept of quasi-doping differs from real doping in that remotely located dopant layers provide mobile electrons, while band gap engineering simulates the potential of the uniform positively charged background. Thus the potential well is essentially free from charged scattering centers, providing a much higher electron mobility within the channel and avoiding carrier localization and freezeout at low temperatures.

The realization of jellium in a real solid is difficult, since in uniformly doped semiconductors the electron-impurity interaction is very strong, leading to the main scattering mechanism presumably at low temperatures, where electron-phonon scattering is small. Pulse-doped semiconductors offer only little improvement in the problem of scattering since here, too, the ionized impurities are in immediate vicinity of the electron system. The introduction of the remote modulation doping technique, however, proved very advantageous and successful in the realization of high mobility quasi-two-dimensional electron systems (2DES). Taking advantage of this fact, it seemed promising to also apply it for a Q3DES. Remote modulation doping of a wide, rectangular quantum well leads to the formation of two isolated 2DES at the two interfaces and is thus not suitable for the realization of a Q3DES. One way out is to artificially grade the potential well, mimicking the potential of a uniform positively charged background. Since in $\text{Al}_x\text{Ga}_{1-x}\text{As}$ in the range of $0 < x < 0.3$ the bandgap depends nearly linearly on the Al content x , spatial variation of x is equivalent to a spatial variation of the conduction band edge. If this spatial variation is chosen to be parabolic, the resulting potential is that of a fictitious charge

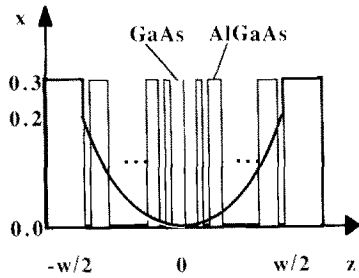


Fig. 1. Sketch of a quasi-doped parabolic well. A 20 Å superlattice consisting of one layer GaAs and one layer $\text{Al}_{0.3}\text{Ga}_{0.7}\text{As}$ of variable duty cycle provides a digital alloy with spatially varying Al content. The parabolic average Al content is given by the solid line.

density given by the curvature of the parabola, namely $n^+ = 8ee_0D/e^2w^2$. Here, D is the energetic height of the parabola from its bottom at $z = 0$ to its edges at $z = \pm w/2$, where w is the width of the well in the growth direction.

In fig. 1 we show a sketch of such a quasi-doped parabolic well. The spatial variation of the Al content is achieved by using a digital alloy technique. Here, we grow a 20 Å period superlattice, each period consisting of one layer GaAs and one layer $\text{Al}_{0.3}\text{Ga}_{0.7}\text{As}$. The duty cycle of these two layers is varied quadratically during the growth, such that the average Al content if integrated over the superlattice approaches the solid line parabola. To the left and the right of the well, dopant layers provide mobile electrons, which act to screen the pseudo-charge and form a Q3DES of space charge density that equals the designed one n^+ . An undoped layer between the dopants and the well reduces ionized impurity scattering and thus enhances the electron mobility in the channel.

To elucidate the actual distribution of free carriers within a quasi-doped parabolic quantum well, we use a capacitance-voltage (CV) profiling technique at room temperature. For this purpose, specially designed samples have been fabricated. Here, the parabolic wells are grown on n^+ -doped substrates with an n^+ -doped cap layer above the well. A Au-Ge electrode evaporated on top of the sample provides a Schottky gate. Between this gate electrode and an In contact on the sample backside, a gate voltage can be applied. The CV measurements then are carried out using an im-

pedance analyzer, operating at a frequency of 1 MHz. By increasing the gate voltage the depletion zone edge beneath the Schottky gate can be swept through the structure, and by measuring the capacitance of the device, an apparent carrier distribution profile as a function of depth into the sample can be extracted. This apparent profile is directly connected with the actual, true electron distribution within the well. Details on this and the deconvolution process used in our calculations will be presented elsewhere. Here, we only wish to point out the results of our investigations. Assuming a quasi-uniform distribution of the free carriers in the well, we can model the expected apparent profile as it would be extracted from CV measurements. Comparison with the experimental data then allows us to fit the true carrier distribution in our samples.

A typical result of such a fit is given in fig. 2, where we plot the measured apparent carrier profile (a) and both the calculated apparent (b) as well as the deduced true carrier profile (c) as a function of the depth beneath the Schottky gate for a 2000 Å wide parabolic well. The true carrier profile is obtained from the best fit of the calcu-

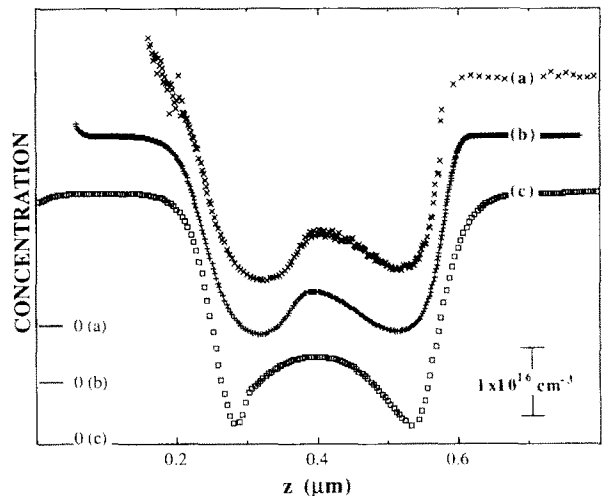


Fig. 2. Typical result of a CV profiling measurement and subsequent deconvolution process. In (a), the measured apparent carrier profile as extracted from the measured capacitance is shown. Assuming a true profile (c), the apparent one (b) is calculated and compared with the experiment. This is done self-consistently, until (a) and (b) coincide.

lated apparent profile to the experimental data. As can be seen, the apparent profile gives a smeared out version of the true one, this smearing occurring over several Debye lengths.

To investigate the electronic properties of the parabolic quantum wells, we measured the electron mobility μ and the carrier concentration N_s in the van der Pauw method. The measurements have been carried out in a temperature range between 300 and 10 K and in magnetic fields up to 0.5 T. The peak mobilities at low temperatures for the samples investigated lie in the range of $\mu = 60\,000 \text{ cm}^2 \text{ V}^{-1} \text{ s}^{-1}$ to $\mu = 200\,000 \text{ cm}^2 \text{ V}^{-1} \text{ s}^{-1}$; a mobility enhancement at low temperatures is clearly visible for all samples. The carrier densities within the wells saturate below about 100 K and lie between $N_s = 1 \times 10^{11} \text{ cm}^{-2}$ and $N_s = 4 \times 10^{11} \text{ cm}^{-2}$ at $T = 12 \text{ K}$. By defining an effective width $w_e = N_s/n^+$ of the Q3DES the wells usually are filled between about 40% to 70% of the nominal well width. Illumination of the samples at low temperatures increases the carrier density due to the persistent photoeffect like in the 2D case, whereas the mobility decreases. This decrease of the mobility with increasing carrier density is attributed to alloy disorder scattering, which increases with increasing Fermi wave vector k_F and turns out to be the dominant scattering process in our samples.

To study the actual distribution of the effective mass in a quasi-doped parabolic quantum well, we measured cyclotron resonance (CR) at $T = 10 \text{ K}$ and in magnetic fields up to 3 T using a Fourier transform spectrometer. For the particular sample that we present here, the lowest Landau levels of the two lowest electrical subbands still are occupied at $B = 3 \text{ T}$. We thus expect the contribution of two subbands to the CR. A typical result of such an experiment is shown in fig. 3a, where we depict the experimental spectrum for $B = 3 \text{ T}$ in Faraday geometry, obtained in a 2000 \AA wide well. The CR lineshape is asymmetric, with a shoulder on the low energy side. This asymmetry has previously also been reported by another group [4]. In fig. 3b, we present the result of a CR lineshape simulation, as obtained by the assumption of the contribution of two subbands to the CR. The influence of the two subbands is repre-

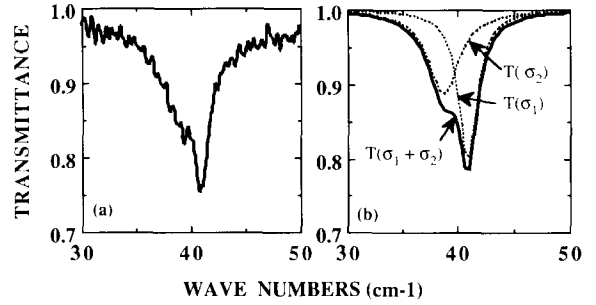


Fig. 3. Experimentally obtained (a) and simulated (b) CR transmission spectrum for a 2000 \AA wide parabolic well. At $B = 3 \text{ T}$ the lowest Landau levels of two subbands are still occupied. The observed CR lineshape is asymmetric, with a shoulder on the low energy side. This is attributed to the influence of a second CR in the higher subband. Parameters for the simulated CR lineshape are $N_s^1 = 1.3 \times 10^{11} \text{ cm}^{-2}$, $\mu_1 = 185\,000 \text{ cm}^2 \text{ V}^{-1} \text{ s}^{-1}$, $m_1^* = 0.0685m_0$ and $N_s^2 = 1.2 \times 10^{11} \text{ cm}^{-2}$, $\mu_2 = 86\,000 \text{ cm}^2 \text{ V}^{-1} \text{ s}^{-1}$ and $m_2^* = 0.0724m_0$ in the higher subband.

sented by two different effective masses $m_{1,2}^*$, two different carrier densities $N_s^{1,2}$ and two different mobilities $\mu_{1,2}$, leading to two calculated CR transmission spectra $T(\sigma_1)$ and $T(\sigma_2)$. Here, $\sigma_i(\omega)$ is the high frequency Drude conductivity in the presence of a magnetic field, and $T(\sigma_i)$ is calculated in an exact electrodynamical way. The resulting lineshape of the CR then is obtained by calculating $T(\sigma_1 + \sigma_2)$. Using the set of parameters given in the figure caption, the agreement between the simulated and the measured CR is very good. The total carrier density $N_s^{\text{tot}} = N_s^1 + N_s^2$ also agrees with the one extracted from van der Pauw measurements. The different masses $m_1^* = 0.0685m_0$ and $m_2^* = 0.0724m_0$ in the two different subbands can be explained by the spatial variation of the Al content within the well. Like the bandgap, also the effective mass in $\text{Al}_x\text{Ga}_{1-x}\text{As}$ depends nearly linearly on the mole fraction x . A parabolic variation of x with depth thus results in a parabolic variation of $m^*(z)$ from $0.067m_0$ in the well center to $0.082m_0$ at its edges, where $x = 0.19$. For simplicity, we assume harmonic oscillator wavefunctions $|\zeta_i\rangle$ and calculate the mean effective mass in the two subbands using $\langle m_1^* \rangle = \langle \zeta_1 | m^*(z) | \zeta_1 \rangle$. The result of this calculation is shown in fig. 4a, where we plot this mean mass for two subbands as a func-

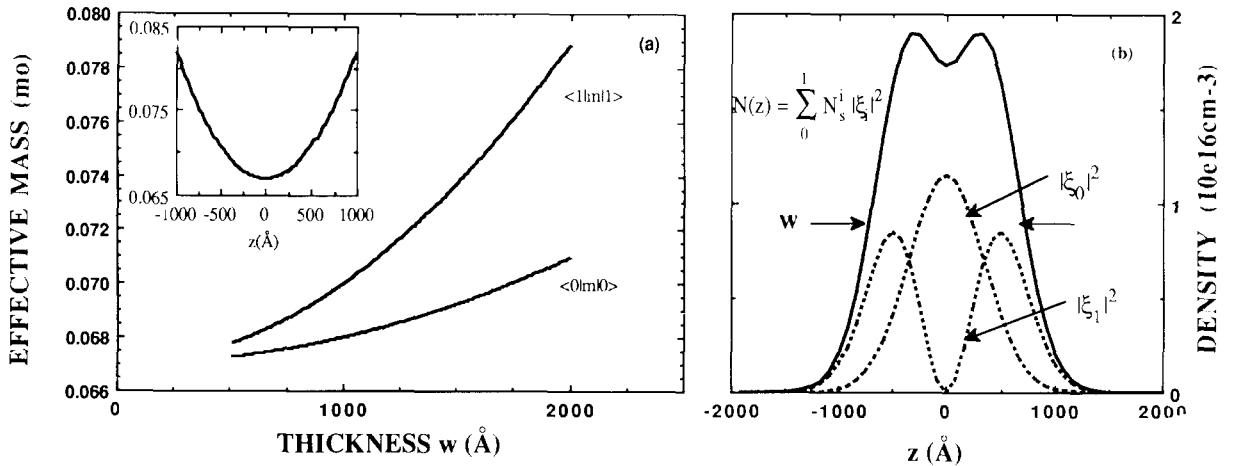


Fig. 4. (a) Effect of a spatially varying Al content on the effective mass in the different subbands. The effective masses are plotted as a function of the width of the Q3DES, as defined in (b). The inset in (a) shows the variation of the effective mass with depth in the graded parabolic well. The effective masses are obtained by calculating the mean masses $\langle m_i^* \rangle = \langle i | m^*(z) | i \rangle$.

tion of the effective width w of the Q3DES. The width w has been defined by the points, where $N(z) = \sum N_s^i |\xi_i|^2$ drops to half its maximum value, as sketched in fig. 4b. An increase in the effective mass is observed for both subbands, if the width of the electron system becomes larger. The increase is more pronounced for the higher subband, which is due to the fact, that the probability density in the higher subband is higher in regions of higher masses. We achieve reasonable agreement between the prediction for the effective masses in this simple model and the experiment, if we assume the width of the Q3DES to be of the order of 1300 Å, which agrees very well with the one extracted from $w_c = N_s/n^+ = 1200$ Å.

In conclusion, we have presented some results of growth and characterization of several quasi three dimensional electron systems, which can be realized in modulation doped graded potential wells. The results of room temperature CV profiling measurements have been used to optimize the growth conditions and thus producing samples with uniform carrier distribution and high electron mobility. The influence of a spatially varying effective mass has been investigated in cyclotron

resonance absorption experiments and can be explained in a simple quantum mechanical model, taking into account the spatial extension of the wavefunctions in different subbands.

We like to thank B.I. Halperin, R.M. Westervelt, and K. Ensslin for fruitful discussions. The FIR measurements have been made possible by the help of V. Jaccarino and coworkers under the SDIO Biomedical and Materials Science Program through the Center for Free Electron Laser Studies. We also wish to acknowledge the U.S. Air Force Office of Scientific Research for financial support under contract # AFOSR-88-0099.

References

- [1] M. Sundaram, A.C. Gossard, J.H. English and R.M. Westervelt, *Superlattices Microstruct.* 4 (1988) 683.
- [2] M. Shayegan, T. Sajoto, M. Santos and C. Silvestre, *Appl. Phys. Lett.* 53 (1988) 791.
- [3] B.I. Halperin, *Jpn. J. Appl. Phys.* 26, Suppl. 26-3 (1987) 1913.
- [4] K. Karrai, H.D. Drew, M.W. Lee and M. Shayegan, *Phys. Rev. B* 39 (1989) 1426.